

Development and *in vitro* characterization studies of novel chitosan nanoparticles for the treatment of Huntington's disease

Emre Şefik ÇAĞLAR¹, Emine Büşra EKER FIDAN², Mehmet Koray GÖK²
Neslihan ÜSTÜNDAĞ OKUR³, Saadet Kevser PABUCCUOĞLU², Erdal CEVHER^{4*}

1 University of Health Sciences, Faculty of Pharmacy, Department of Pharmaceutical Biotechnology, Istanbul, Türkiye

2 Istanbul University-Cerrahpasa, Faculty of Engineering, Department of Chemical Engineering, Istanbul, Türkiye

3 University of Health Sciences, Faculty of Pharmacy, Department of Pharmaceutical Technology, Istanbul, Türkiye

4 Istanbul University, Faculty of Pharmacy, Department of Pharmaceutical Technology, Istanbul, Türkiye

ABSTRACT

Huntington's disease is a fatal disease that occurs when the number of CAG trinucleotides in the IT-15 gene repeats itself more than 35 times. In this study, modified chitosan polymers were synthesized and characterized. siRNA loaded nanoparticles were prepared and characterized. The results showed that the modified chitosan was successfully synthesized and targeted. As a result of the characterization studies, the particle size, polydispersity index and zeta potential of the siRNA-loaded nanoparticle were found to be 99.0 ± 5.1 nm, 0.3190 ± 0.004 , and 14.9 ± 3.04 mV, respectively. Lyophilization was successfully achieved with a trehalose rate of 20%. As a result of 12 months of stability, the particle size of the formulations was found to be the highest 273.766 ± 8.957 nm, the highest polydispersity index was 0.324 ± 0.016 , and the highest zeta potential was 45.35 ± 1.79 mV. In agarose gel electrophoresis studies, the siRNA:modified chitosan ratio was found to be 5:1. siRNA-loaded nanoparticles maintain the integrity of siRNA for 24h.

Keywords: Huntington's disease, siRNA, chitosan, nanoparticle

*Corresponding author: Erdal Cevher

E-mail: ecevher@istanbul.edu.tr

ORCID:

Emre Şefik ÇAĞLAR: 0000-0003-2010-4918

Emine Büşra EKER FIDAN: 0000-0002-6340-5107

Mehmet Koray GÖK: 0000-0003-2497-9359

Neslihan ÜSTÜNDAĞ OKUR: 0000-0002-3210-3747

Saadet Kevser PABUCCUOĞLU: 0000-0002-1793-0859

Erdal CEVHER: 0000-0002-0486-2252

(Received 12 Jan 2025, Accepted 10 Feb 2025)

INTRODUCTION

Huntington's disease (HD) is a progressive neurological condition resulting from the expansion of CAG repeats that encode polyglutamine at the N-terminus of the huntingtin protein. The HD gene (IT-15) spans 180 kb and is classified into four categories according to the quantity of CAG repeats. Individuals possessing 26 or fewer repeats are considered healthy, whereas those with 27 to 35 repeats exhibit intergenerational instability. Those who are more than 35 synthesize the disease protein. The striatum is the predominant brain area associated with instability, experiencing particular deterioration^{1,2}.

HD induces involuntary movements, motor coordination impairments, cognitive decline, and psychiatric issues. The pathogenic characteristic is the selective death of neurons in the basal ganglia of the brain. Symptoms encompass weight reduction, muscular debilitation, metabolic irregularities, and endocrine abnormalities. Atrophy is evident in multiple brain regions, particularly in severe instances³.

HD, which is autosomal dominant; In American, European, and Australian societies, it affects about 5-10 out of every 100,000 people in the white race^{4,5}. The age of onset of the disease may vary from childhood to the end of eighty years of age⁶. However, the most common age range of the disease is between 30-50⁵. The average time between the occurrence of the disease and death is between 17-20 years^{5,6}.

Treatment is carried out by symptomatic treatment of motor, behavioral, and psychiatric disorders. There is still no drug that modifies the disease^{5,6}. Unfortunately, current pharmacotherapy in HD does not offer anything beyond temporary relief of symptoms and fails to stop both the underlying cause and progression of the disease. Therefore, it is very important to better provide standard care for Huntington's patients and to develop a new treatment strategy that will stop the progression of the disease.

RNA interference (RNAi) is a rapidly evolving field in biological research, potentially treating certain diseases by blocking protein production by inhibiting or degrading mRNA translation or degrading mRNA. This intracellular pathway allows cells to regulate gene expression through microRNAs, playing a crucial role in development^{7,8}. siRNAs are loaded on RNA-based silencing complex (RISC), activated by thermodynamic selection or siRNA expansion. RISC targets specific complementary mRNA transcriptions, preventing protein production, and catalyzing numerous chain reactions, increasing the potency of gene silencing compared to ASOs^{9,10}.

The main pathways for transport from the nose to the brain are olfactory epithelium, olfactory nerve, and blood circulation. The olfactory nerve pathway is formed by fusion of olfactory sensory nerve axons. It travels from the ethmoid bone to the cranial cavity, where it makes synoptical unions with *epiplexus* and mitral cells in the olfactory bulb. Drug molecules remain in the olfactory mucosa after intranasal administration, passing through olfactory epithelial cells and accumulating in Bowman's gland and Sertoli cells in the brain. They also pass through intercellular gap junctions and accumulate in brain tissues. Chitosan, which is a semi-natural cationic biopolymer, offers advantages like biocompatibility, biodegradability, low toxicity, easy preparation, and high loading capacity for hydrophilic drugs, making it a useful carrier for plasmid DNA, siRNA, and cancer drugs¹¹. PEGylation is a recognized method for circumventing the elimination of nanoparticles by macrophages. This technique involves coating nanoparticle surfaces with an anti-fouling polymer, such as polyethylene glycol, which is non-toxic and non-immunogenic; this process is referred to as "PEGylation." PEGylation also entails the alteration of the dimensions and morphology of nanoparticles. PEGylation of nanoparticles has been identified as an effective strategy for prolonging nanoparticle circulation time while evading liver macrophages. PEGylation forms a hydrophilic barrier surrounding nanoparticles, safeguarding connections between complement proteins and immunoglobulins (opsonin proteins) through steric repulsion forces, therefore obstructing and postponing the early phase of the opsonization process. Consequently, PEGylation has demonstrated a significant enhancement in the circulatory half-life of nanoparticles by multiple orders of magnitude¹². For this reason, nanoparticles were PEGylated. In addition, since the number of N-methyl-D-aspartic acid (NMDA) receptors in HD is increasing, the developed nanoparticles have been targeted with NMDA¹³.

For instance, Sava et al. found the particle size and zeta potential of siRNA-loaded chitosan nanoparticle formulations developed for use in the treatment of HD between 103.7-205 nm and 42.5-54.7 mV, respectively. As a result of the study, when intranasally administered siRNA-loaded chitosan nanoparticles were compared with intranasally administered siRNA, they found that siRNA-loaded chitosan nanoparticles inhibited the synthesis of mutant huntingtin protein at a rate of 77% compared to siRNA¹⁴.

This study aims to demonstrate the effectiveness of siRNA-loaded modified chitosan nanoparticles in treating HD, as a new treatment and to enhance the effectiveness and reduce side effects of current treatments.

METHODOLOGY

Materials

Human siRNA Oligo Duplex (siRNA), trilencer-27 fluorescent-labeled trans, siTran 2.0 siRNA transfection reagent were purchased from Oligogene (USA). Low molecular weight chitosan (Chi) (75-85% deacetylated), gallic acid (GA), 3-dimethylamino-1-propylchloride hydrochloride (DAPC), N-(3-dimethylaminopropyl)-N'-ethylcarboimide hydrochloride (EDAC), acetic acid, sodium hydroxide (NaOH), methoxy-PEG 2000 (MPEG), isopropanol, sodium acetate, phosphate buffer solution (PBS) tablets, tris base, EDTA, agarose, ethidium bromide (EtBr), and bromophenol blue, in tris-acetate-EDTA buffer (TAE), tris-borate-EDTA (TBE), N-methyl-D-aspartic acid (NMDA) were purchased from Sigma Aldrich (Germany). Sodiumtripolyphosphate (TPP), ethanol, fetal bovine serum (FBS), were purchased from Merck (Germany).

Methods

Synthesis of PEGylated and targeted of chitosan polymers

Firstly, Chi-GA was synthesized by the reaction between Chi and GA, then Chi-GA product was reacted with DAPC for the preparation of the Chi-GA-DAPC product. Afterwards, Chi-GA-DAPC product was pegylated using MPEG and Chi-GA-DAPC-MPEG product was obtained. Finally, Chi-GA-DAPC-MPEG product was targeted with NMDA for the preparation of the targeted product Chi-GA-DAPC-MPEG-NMDA.

Chi was dissolved in 4% acetic acid solution as 1% (w/v). GA (1 mole of GA per 1 mole of glucosamine unit) was dissolved in 10 mL of ethanol and EDAC was used to activate the carboxylic acid groups of GA. Since the concentration of Chi to be used in the synthesis is very high and the high solubility of Chi is desired, the acetic acid concentration has been determined as 4% to obtain high solubility of Chi. The mixture was stirred at room temperature for 24 hours, and the pH was adjusted to 8.5-9.0 with 1 N NaOH for the precipitation of Chi-GA product. To purify the Chi-GA, the precipitated product was centrifugated and washed. Synthesis of the Chi-GA-DAPC product was realized by the reaction of Chi-GA with DAPC in alkaline pH 8.5-9. In addition, DAPC (0.5 moles of DAPC per 1 mole of GA modified glucosamine unit) was dissolved in 1.176 mL of isopropanol and this solution was added to the Chi-GA solution at a rate of 168 μ L every 5 minutes and mixed for a period of 30 minutes. The mixture was stirred at 500 rpm for 4 h, and at the end of the incubation period, 60 mL of technical ethanol was added to stop the reaction.

Pegylation of the Chi-GA-DAPC, this product was dissolved in 1% acetic acid, and MPEG was added to the solution. The mixture was stirred 50°C for 48 hours, dialyzed against deionized water for 24 hours, and lyophilized at $-50 \pm 1^\circ\text{C}$ at a pressure of 0.01 mBar. The purified Chi-GA-DAPC-MPEG product was stored at $+4^\circ\text{C}$. To obtain the targeted polymer Chi-GA-DAPC-MPEG-NMDA, Chi-GA-DAPC-MPEG was dissolved in 4% acetic acid, and NMDA (0.02 mol NMDA per 1 mole of glucosamine unit) was dissolved in ethanol, then this solution was activated with EDAC. EDAC-activated NDMA solution was added to the Chi-GA-DAPC-MPEG solution, mixed under the N_2 gas for 24 hours, and the pH adjusted to 8.5-9 for the precipitation of the product. The Chi-GA-DAPC-MPEG-NMDA product was purified by centrifuging at 6000 rpm for 5 minutes, washed with deionized water, and lyophilized at $-50 \pm 1^\circ\text{C}$ ¹⁵.

Characterization of synthesized polymers

Determination of molecular weight of polymers

The study aimed to determine the molecular weight and molecular weight distributions of suitable polymers for nanoparticle preparation using the Gel Permeation Chromatography (GPC) method. The TOSOH EcoSEC branded GPC/SEC system was used to determine the average molecular weights and molecular weight distributions of modified polymers. The study used chitosan and modified chitosan products, which were dissolved overnight in a 1% acetic acid solution, diluted twice with sodium acetate, filtered through a 0.22 μm membrane, and transferred to vials¹⁶.

Determination of structural properties of polymers

The structural properties of the synthesized polymers were investigated by Fourier Transform Infrared (FT-IR) Spectroscopy, ^1H NMR and ^{13}C NMR analyzes.

Fourier Transform Infrared Spectrophotometry (FT-IR)

The structures of all synthesized products were illuminated by Fourier Transform Infrared Spectrophotometer technique. FT-IR analyses showed that the Cary 630 model (Agilent; USA) on the FT-IR device. Using tablets diluted with a product/KBr ratio of 1/200 mg, the spectra was recorded in the wavenumber range of 650-4000 cm^{-1} .

Nuclear Magnetic Resonance (^1H -NMR and ^{13}C -NMR)

In addition to the FT-IR method, the UNITY INOVA nuclear magnetic resonance spectrophotometer (Varian, Canada) was used to elucidate the structures of their products. Analyses were performed using MSO - d₆:D₂O solvents and 500 MHz and 25°C parameters.

Thermal analysis

Thermogravimetric analysis (TGA) was performed to determine the thermal degradation properties of the synthesized polymers. For this purpose, TGA analysis of the samples (15 mg) placed in aluminum crucible was carried out with a thermogravimetric analyzer (Linseis, STA PT 1750 model, USA) with a heating rate of 10°C/minute up to 1000°C by sending air into the system at a speed of 0.4 L/min.

Preparation and characterization of siRNA-loaded chitosan nanoparticles

Positively charged modified chitosan nanoparticles were prepared by ionic gelation technique using tripolyphosphate¹⁷. Stock chitosan solutions of 0.3% were prepared for the preparation of nanoparticles obtained from modified Chi polymers. Nanoparticles were obtained using a 0.1% TPP solution. The final concentration of 0.025% with the synthesized polymers was studied as shown in Table 1 with a Chi:TPP ratio of 6:1 for 5 mL Chi nanoparticles. TPP was added drop by drop to the Chi solution stirring at 300 rpm, with 3 seconds between each drop.

Table 1. Preparation of modified Chi nanoparticles

Formulation Codes	Modified Chi solution (mL)	Modified Chi TPP Ratio	TPP solution (mL)	Water (mL)
Chi-GA-DAPC Chi-GA-DAPC-MPEG Chi-GA-DAPC-MPEG-NMDA	0.417	6:1	0.208	4.375

The procedure applied for all modified Chi polymers.

The siRNA added to the nanoparticle by ionic interaction method. For this, the first nanoparticles were prepared as mentioned. Afterwards, for 30 min, nanoparticle and siRNA together stirred at 50 rpm.

Particle size, PDI and surface charges of nanoparticles

The particle size and poly dispersity index (PDI) of the nanoparticles were determined using the photon correlation spectroscopy method (Malvern Zetasizer, Nano-ZS). The zeta potential of the formulations was investigated with a Malvern Zetasizer at 25°C, 78.5 dielectric constant, 5 mS/cm conductivity, using DTS 1060C zeta cuvette, and 40 V/cm field power¹⁸.

Lyophilization of formulations and moisture determination

After the addition of cryoprotectant (trehalose) at different ratios (5%, 10%, 20%, 40%), 5 mL of formulations were frozen in 10 mL glass vials in the freezer at -20°C for 2 hours. Then, it was lyophilized with a VirTis AdvancePlus brand lyophilizer device under 17 mTorr pressure at -45°C for 48 hours.

The lyophilized samples were re-dispersed and analyzed by measuring particle size, particle distribution and zeta potential at certain time intervals for 4 hours. All measurements are the result of at least 3 parallel studies and the measurement has been repeated at least 5 times.

For moisture determination studies, lyophilized formulations were carefully weighed to determine the initial weight (IA). They were then heated in an oven from 30°C to 100°C. They were immediately weighed, and their final weight (FA) was found⁹. The % moisture content is calculated according to the following formula:

Equation 1. % moisture content determination

$$\text{Moisture (\%)} = \frac{\text{IA-FA}}{\text{IA}} \times 100$$

Agarose gel electrophoresis studies

The study investigated the stability of siRNA loaded on nanoparticles in a formulation using agarose gel electrophoresis. The agarose was dissolved in tris-acetate-EDTA buffer (TAE), then EtBr was added. The gel was then placed in a tank with pH 8.0 TAE buffer and optionally mixed with 6x agarose gel loading dye. The electrophoresis process was completed in 1 hour at 100 V. The gels were then examined on a UV transilluminator¹⁶.

Evaluation of serum stability of nanoparticles

The study demonstrates the integrity of siRNA nanoparticles at different time intervals using polyacrylamide gel electrophoresis. The nanoparticle formulation was enriched with 5% FBS, and 30 µL samples were taken at different times and stored at -20°C. Heparin was added to the formulations and waited for 1 hour for siRNA separation. The integrity of the siRNA was analyzed using 20% polyacrylamide gel electrophoresis stained with 1% EtBr. The gel was prepared by mixing 40% acrylamide with 10X TBE buffer and distilled water, adding ammonium persulfate and tetramethylethylenediamine, and applying electrophoresis loading buffer with 6x agarose gel loading dye. Samples were conducted for 30 minutes at 200V amperes, and the gel was kept in TBE buffer

containing 1% EtBr for 30 minutes. The gels were then examined on a UV transilluminator for polyacrylamide gel^{20,21}.

Stability studies

Lyophilized Chi-GA-DAPC-MPEG-NMDA formulations were stored in a stability cabinet at 0, 3, 6, 9, and 12 months at $4 \pm 2^\circ\text{C}$ (in the refrigerator), $25 \pm 2^\circ\text{C}$ and $60 \pm 5\%$ relative humidity and $40 \pm 2^\circ\text{C}$ and $75 \pm 5\%$ relative humidity to measure particle size, polydispersity index, and zeta potentials. Stability studies were carried out in accordance with the ICH Guidelines²².

RESULTS and DISCUSSION

Molecular weight determination studies of synthesized polymers

The results of the determination of molecular weights of Chi-GA-DAPC-MPEG, Chi-GS-DAPC-MPEG-NMDA polymers are shown in Table 2. When the molecular weights of Chi-GA-DAPC-MPEG polymer and the related PDI results were examined, it was seen that the Chi-GA-DAPC-MPEG obtained as a result of this study were in appropriate weights and showed a very good distribution (monodisperse). The average molecular weight of the Chi, which is commercially sold as “low molecular weight” by Sigma, which was obtained in previous studies, is 284.0 ± 2.9 kDa and the PDI is 2.62 ± 0.05 , which confirms our result¹⁵. However, the reason why the molecular weight of Chi-GA-DAPC-MPEG polymers is lower than the molecular weight of commercially sold Chi is thought to be that the chains of Chi are broken due to temperature and environmental factors during the modifications made, and then purification and removal processes are applied¹⁵.

Table 2. Average molecular weight determination results of modified Chi polymers

Formulation	M_n (kDa)	M_w (kDa)	PDI (M_w/M_n)
Chi-GA-DAPC-MPEG	92.00 ± 0.53	99.00 ± 0.66	1.079 ± 0.01
Chi-GA-DAPC-MPEG-NMDA	31.84 ± 0.25	40.79 ± 0.27	1.281 ± 0.370

Determination of structural properties of polymers

FT-IR spectra

A careful comparison of the Chi-GA-DAPC-MPEG and the Chi-GA-DAPC-MPEG-NMDA FTIR spectra presented in Figure 1 indicates definite differences about some absorption bands related to the reactions.

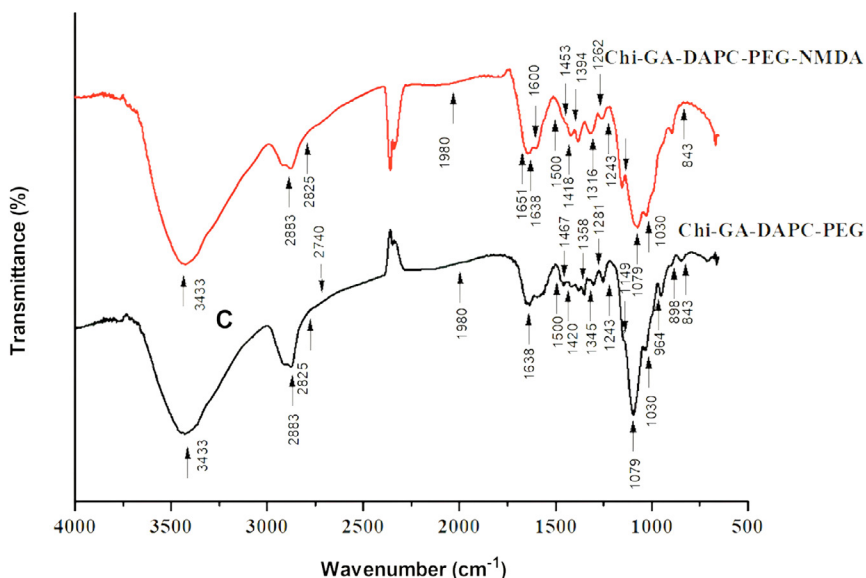


Figure 1. FT-IR spectra of Chi-GA-DAPC-MPEG and Chi-GA-DAPC-MPEG-NMDA

When the FT-IR spectra (Figure 1) were evaluated, new secondary amide structure formation by the reaction between the primary amine (NH_2) group of Chi-GA-DAPC-MPEG and the carboxyl (COOH) group in NMDA molecule was observed at about max. 1651 cm^{-1} corresponding to the stretching vibrations of the Amide I $\text{C}=\text{O}$ bonds. It has also been observed that formation of the new ester structures (at about max. 1600 , 1418 , 1394 , and 1316 cm^{-1} corresponding to the stretching vibrations of the $\text{C}-\text{O}/\text{C}=\text{O}$ bonds in the ester structure) by the reaction between the COOH groups of NMDA molecule and the unreacted methylol groups on the Chi skeletal structure or the free OH group in the MPEG structure.

The data obtained according to the FTIR spectra results show that the Chi-GA-DAPC-MPEG-NMDA product were successfully synthesized as expected.

Nuclear Magnetic Resonance ($^1\text{H-NMR}$ and $^{13}\text{C-NMR}$)

As a result of the structural characterization of Chi, Chi-GA-DAPC-MPEG and Chi-GA-DAPC-MPEG-NMDA polymers with $^1\text{H-NMR}$ and $^{13}\text{CNMR}$ spectroscopy of selected polymer Chi-GA-DAPC-MPEG-NMDA by performing the reactions with MPEG and NMDA, it was seen that the reactions took place as expected (Figure 2). Accordingly, the intense observance of the peaks of protons belonging to the ($-\text{O}-\text{CH}_2-\text{CH}_2$) groups around 3.5 ppm in the Chi-GA-DAPC-M-PEG graph showed that PEGylation reactions took place suc-

cessfully. However, in these spectra, it was observed that the peaks of protons belonging to the groups around 3.2 ppm and 1.9 ppm ($\text{NH-CH}_2\text{-CH}_2\text{-NH-CH}_2\text{-CH}_2\text{-N-CH}_3\text{-CH}_3\text{-CH}_3$) originating from DAPC compounds disappeared in the Chi-GA-DAPC-MPEG-NMDA graphs and/or interfered with other peaks, and a reaction took place between the unreacted methylol groups of Chi skeletal structure and NMDA.

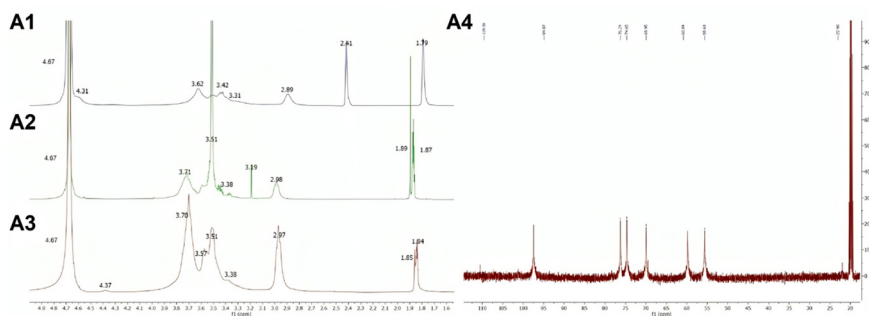


Figure 2. A1) Chi; A2) Chi-GA-DAPC-MPEG, A3) $^1\text{H-NMR}$ Spectrum of Chi-GA-DAPC-MPEG-NMDA polymers, A4) $^{13}\text{C-NMR}$ Spectrum of Chi-GA-DAPC-MPEG-NMDA polymer, Chi-GA-DAPC-MPEG-NMDA polymer, $^{13}\text{CNMR}$ (125 MHz, Acetic acid- d_4 ; $\delta = 19.99$) [ppm]: $\delta = 22.03$; 55.62; 55.66; 59.79; 69.47; 69.95; 74.65; 76.24; 97.47; 110.53.

The results were found to be consistent with the results of FT-IR analysis.

Thermal analysis

The data obtained from the TGA curves of Chi-GA-DAPC-MPEG and Chi-GA-DAPC-MPEG-NMDA polymers obtained by this study are given in Table 3. First, the TGA curves of Chi-GA-DAPC-MPEG polymer and the weight losses and final degradation temperatures obtained from these curves are given. In the range of approximately 115 to 208°C, corresponding to the initial degradation stage, a significant weight loss of 10% was observed for Chi-GA-DAPC-MPEG-NMDA and Chi-GA-DAPC-MPEG, respectively. The middle stage took place in the temperature range of approximately 328-415°C with a weight loss of approximately 60-80% depending on the modified polymer structures and the main weight losses were observed at this stage. The final oxidative degradation was completed at approximately 589-760°C due to modified products structures.

Table 3. The weight losses (%) and the final degradation temperatures obtained from TGA data curves of Chi-GA-DAPC-MPEG, Chi-GA-DAPC-MPEG-NMDA polymers

Weight Loss* (%)	Temperature (°C)	
	Chi-GA-DAPC-MPEG	Chi-GA-DAPC-MPEG-NMDA
5	113	86
10	208	115
20	248	267
50	313	338
100	589	760

*Values calculated from TGA curves

As shown in Table 4, the thermal oxidative degradation properties of Chi-GA-DAPC-MPEG-NMDA exhibit the same behavior. The decomposition of the polymer in air occurs in 4 stages, at temperature ranges very close to each other. Table 3 shows the degradation stages, temperature ranges, corresponding maximum weight loss % amounts and final degradation temperatures of polymer. The polymer showed a weight loss of approximately 5-15% in the initial degradation interval due to the removal of the trapped water in their molecules. Subsequently, until the end of stage 2, the rate of degradation is very slow, and no significant weight loss is observed up to 200-270°C and maintains values of 10-15%. Stage 3 is the fastest step in degradation and a weight loss ranging from 47-65% is achieved in this region. Subsequently, the rate slows down in the final degradation zone and the degradation ends at 650°C for the last two products and at 760°C, which is the higher temperature for the other product, with the formation of CO, CO₂, and similar gases. As a result, it is clearly seen that the attachment of NMDA ligand to chitosan-based modified products does not adversely affect its thermal oxidative resistance²³.

Table 4. Degradation stages of Chi-GA-DAPC-MPEG-NMDA

Polymer	Chi-GA-DAPC-MPEG-NMDA	
Degradation stage	Temperature range (°C)	Weight loss* (%)
1	25-120	10
2	120-270	15
3	270-300	47
4	300-760	100
Final degradation temperature (°C)	760	

* Values calculated from TGA curves

Preparation of nanoparticles and results of characterization

The particle size and size distribution PDI of the nanoparticles were determined using the photon correlation spectroscopy method. Nanoparticle formulations are ideally selected based on their particle size, size distribution, and zeta potential. Of the ideally selected nanoparticle formulations, the smallest ones were determined as those with a particle distribution of 0.5 and below, and those with a zeta potential of +30mV and above. Table 5 shows the particle size, PDI, and zeta potential results of the formulations determined as ideal. As a result of these evaluations, it is aimed to obtain nanoparticle formulations that cross the blood brain barrier (BBB) without being attached to the reticuloendothelial system, show homogeneous distribution, can be loaded with all siRNA and have no toxic effects²⁴⁻²⁶.

Table 5. Particle size, PDI, zeta potential results of blank, and siRNA loaded formulations

Formulation Code	Particle Size (nm) ± SD	PDI ± SD	Zeta Potential (mV) ± SD
Chi-GA-DAPC	165.5 ± 2.6	0.343 ± 0.036	38.8 ± 1.4
Chi-GA-DAPC-MPEG	131.8 ± 9.0	0.311 ± 0.010	29.8 ± 1.0
Chi-GA-DAPC-MPEG-NMDA	146.8 ± 1.1	0.236 ± 0.011	45.3 ± 0.1
Chi-GA-DAPC-MPEG-NMDA-siRNA	99.0 ± 5.1	0.319 ± 0.004	14.9 ± 3.0

The PDI value of null and siRNA-loaded nanoparticle formulations was found to be substantially less than 0.5.

The surface composition of nanoparticles is essential for identifying cell entry mechanisms. It is explained that a highly positive surface charge shows a different bio-dispersion than a slightly negative nanoparticle surface charge. Small particle size and positive surface charge are physicochemical properties that aid cellular uptake by facilitating interactions with the negatively charged cellular membrane^{27,28}.

For nasal to brain drug administration, the size of the ideally sized nanoparticles should be smaller than 200 nm. The particle size of the prepared delivery systems plays an important role in the formulation development and characterization phase as it affects activities such as drug release, biodistribution, cell uptake, etc. Accordingly, Mantimadugu et al. prepared polymeric nanoparticles with a particle size of ≈ 200 nm (139.52 ± 5.35 nm) and provided direct passage to the brain by transcellular transport along olfactory axons²⁹.

Several studies have shown a clear inverse correlation between nanoparticle size and BBB penetration^{30,31}. Most of the studies in animal models of stroke and Parkinson's so far have used nanoparticles with sizes between 50 nm and 100 nm. Godinho et al. revealed that the low size (a hydrodynamic diameter between 100 nm and 350 nm) and positive surface charge of β -Cyclodextrin siRNA nano transporter formulations make them ideal for targeting to the brain³².

The fact that the PDI value was less than 0.5 showed that the particle size distribution of the prepared formulations was homogeneous¹⁸. Van Woensel et al. prepared siRNA-loaded chitosan nanoparticles for the treatment of glioblastoma. Particle sizes, particle distribution, and zeta potential were found to be 141 ± 5 nm, 0.3, and + 32mV, respectively. As a result of the study, it has been shown that chitosan nanoparticle formulations administered intranasal route carry siRNA to the central nervous system in a short time³³.

Furthermore, the positive zeta potential can improve the stability of nanoparticles intended to be used for siRNA administration. Nanoparticles with medium (up to 15 mV) or high positive zeta potential (above 15 mV) can cross the BBB and have been found to be effective as drug-delivery systems to the brain. For example, Jalluli et al. identified cationic nanoparticles prepared with maltodextrin, which has a high positive zeta potential, as effective in brain transport. In addition, high negative/positive (15 to 30 mV) values of the zeta potential prevent coalescence between particles, stabilizing nanoparticle dispersion due to electrostatic repulsions³⁴. When the studies were evaluated, the particle size, particle distribution, and zeta potential of our chitosan nanoparticle formulations were suitable for intranasal application.

Lyophilization studies

Freeze drying is a good technique to improve the long-term stability of colloidal nanoparticles. The poor stability of nanoparticles in an aqueous medium is a major obstacle to their clinical use^{35,36}. The use of trehalose, mannitol or sorbitol as a cryoprotectant is an effective way to maintain the physical properties of nanoparticles during freeze-drying^{37,38}. Among these cryoprotectants, one of the most preferred is trehalose³⁹⁻⁴¹. The non-toxicity of trehalose increases its preferability⁴². Almalik et al. prepared chitosan nanoparticles by ionic gelation method. They investigated the stability of these systems in terms of particle size using six different cryoprotectant species (sucrose, glucose, trehalose, mannitol, polyethylene glycol-2000, and polyethylene glycol-10.000) at concentrations of 5%, 10%, 20%, and 50%. They found that the cryoprotectants of sucrose and trehalose had the highest protective effect in chitosan nanoparticles⁴³. As a result of all the optimization studies, the lyophilization of nanoparticle formulations has been successful (Table 6). When the formulations were evaluated, the ideal cryoprotectant ratio was found to be 20%. However, lyophilized formulations were deposited in stability cabinets for 12 months to evaluate their stability.

Table 6. Particle size, polydispersity index and zeta potential values obtained as a result of redispersing formulations containing 20% D-(+)-trehalose

Time (min)	Particle Size (nm) \pm SD	PDI \pm SD	Zeta Potential (mV) \pm SD
Chi-GA-DAPC-MPEG-NMDA			
0	188.1 \pm 9.5	0.290 \pm 0.010	48.9 \pm 0.7
5	203.1 \pm 7.7	0.329 \pm 0.066	55.3 \pm 0.4
15	208.1 \pm 0.0	0.338 \pm 0.027	53.2 \pm 1.5
30	222.6 \pm 11.4	0.268 \pm 0.044	52.5 \pm 1.2
60	207.5 \pm 0.0	0.275 \pm 0.027	49.1 \pm 0.2
120	229.9 \pm 4.4	0.216 \pm 0.182	51.0 \pm 0.1
180	201.0 \pm 10.1	0.247 \pm 0.002	53.8 \pm 2.4
240	200.5 \pm 2.7	0.283 \pm 0.033	52.5 \pm 0.9

Moisture determination of Chi-GA-DAPC-MPEG-NMDA formulation was performed. Determination of moisture content in lyophilized formulations is essential for predicting the quality and stability of freeze-dried products⁴⁴. In the determination of moisture amount of lyophilised Chi-GA-DAPC-MPEG-NMDA, moisture (%) was determined as 0.558%. For this reason, they found that the lyophilization technique used was a suitable and sufficient method to obtain dry powder.

Stability studies

When the twelve-month stability study was evaluated, it was observed that there were no major changes in particle size, polydispersity index and zeta potential of Chi-GA-DAPC-MPEG-NMDA formulation. For this reason, it is predicted that the prepared chitosan nanoparticles can be stored in a lyophilized manner. The improved stability provided by the removal of water is used extensively by the pharmaceutical industry⁴⁴. Üstündağ Okur et al. prepared nebivolol-loaded solid lipid nanoparticles and modified the nanoparticles with chitosan and PEG. They lyophilized the prepared nanoparticle dispersions by adding 11% trehalose. Then, they examined the effects of lyophilization on particle size, PDI, and zeta potential and determined the amount of moisture in nanoparticles after lyophilization. Particle size growth was seen in unmodified nanoparticles, but not specifically in chitosan and PEG-modified nanoparticles⁴⁵.

Table 7. Evaluation of the 12-month stability study of formulations in terms of particle size, polydispersity index and zeta potential

Time (month)	Chi-GA-DAPC -MPEG-NMDA-4°C			Chi-GA-DAPC -MPEG-NMDA-25°C			Chi-GA-DAPC -MPEG-NMDA-40°C		
	Particle Size (nm) ± SD	PDI ± SD	Zeta Potential (mv) ± SD	Particle Size (nm) ± SD	PDI ± SD	Zeta Potential (mv) ± SD	Particle Size (nm) ± SD	PDI ± SD	Zeta Potential (mv) ± SD
0	243.8 ± 17.1	0.322 ± 0.054	49.5 ± 1.4	243.8 ± 17.1	0.322 ± 0.054	49.5 ± 1.4	243.8 ± 17.1	0.322 ± 0.054	49.5 ± 1.4
3	247.6 ± 5.2	0.333 ± 0.005	48.0 ± 3.6	241.9 ± 0.2	0.266 ± 0.035	45.0 ± 2.6	243.1 ± 1.6	0.393 ± 0.001	45.4 ± 3.3
6	239.2 ± 5.1	0.291 ± 0.013	40.9 ± 0.7	220.3 ± 1.6	0.382 ± 0.140	43.3 ± 1.3	196.6 ± 7.6	0.347 ± 0.042	34.6 ± 1.0
9	241.4 ± 11.9	0.333 ± 0.024	45.0 ± 0.6	252.2 ± 4.4	0.344 ± 0.087	44.8 ± 2.6	259.5 ± 7.9	0.303 ± 0.022	41.8 ± 2.4
12	273.8 ± 8.9	0.287 ± 0.024	43.63 ± 1.1	263.3 ± 3.1	0.309 ± 0.035	45.35 ± 1.8	270.8 ± 7.9	0.324 ± 0.016	45.3 ± 1.0

The evolution of size during storage is ascribed to multiple factors, such as particle aggregation that promotes effective rearrangement, the interaction of free polymer chains with the particle network leading to the reorganization of intermolecular entanglements, syneresis, and swelling induced by TPP, which causes water influx via osmosis. The identical condition has been noted in the developed formulations. Consequently, as the nanoparticles underwent reorganization over time, the particle size initially diminished and subsequently rose, exhibiting no substantial variation, as illustrated in Table 7.

Agarose gel electrophoresis studies

The polymer:siRNA ratio was determined by calculating milligrams of polymer and gene per microliter. The results of agarose gel electrophoresis are shown in Figure 3. As a result of the study, it was found that the polymer: siRNA retention ratio was 5:1 for for Chi-GA-DAPC-MPEG-NMDA. In this study, the desire is that the siRNA does not emit any radiation during imaging. In this way, it is proven that siRNA is retained by the prepared formulations. The results of the study are consistent with the literature⁴⁶.

1	2	3	4	5	6	7
siRNA	Chi-GA-DAPC-MPEG-NMDA					
0.1µg	3:1	5:1	7:1	10:1	12:1	20:1
						

Figure 3. Gel electrophoresis images of nanoparticle formulations derived from Chi-GA-DAPC-MPEG-NMDA

Serum stability results of siRNA-loaded nanoparticles

Nanoparticles interact with various biological environments, including proteins and ions, affecting their physicochemical properties. These interactions can significantly alter colloidal stability and physicochemical properties. However, these interactions can sometimes be overlooked, making it crucial to understand their impact on drug transport, as they can significantly alter the physicochemical properties, colloidal stability, and nanoparticle-cell interactions⁴⁷. The study examined the stability of nanoparticles in serum, predicting

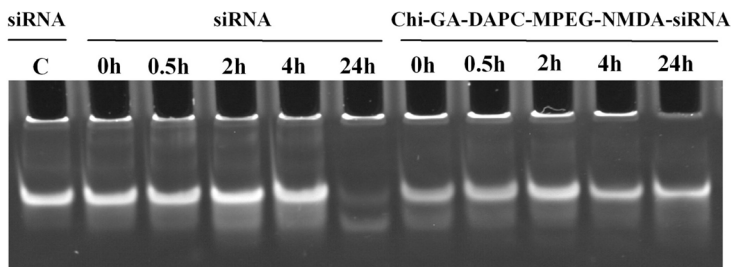
they might enter the bloodstream through intranasal administration. Table 8 shows the changes in particle size, PDI value, and zeta potential, and siRNA integrity was examined over time by using polyacrylamide gel electrophoresis.

Table 8. Particle size, size distribution and zeta potential values of nanoparticles in the presence of 5% FBS

Chi-GA-DAPC -MPEG-NMDA			
Time (h)	Particle Size (nm) ± SD	PDI ± SD	Zeta Potential (mv) ± SD
0	235.3 ± 8.4	0.349 ± 0.049	53.6 ± 2.9
0.5	586.8 ± 36.4	0.812 ± 0.032	12.8 ± 0.1
2	733.7 ± 20.1	0.695 ± 0.180	10.3 ± 0.2
4	770.2 ± 53.0	0.275 ± 0.054	9.85 ± 0.4
24	785.5 ± 11.8	0.263 ± 0.028	10.3 ± 0.2

The size, PDI value and zeta potential of the Chi-GA-DAPC -MPEG-NMDA nanoparticle were found to be 235.3 ± 8.4 nm, 0.349 ± 0.049, and 53.6 ± 2.9 mV, respectively. As the process progressed, the zeta potential of the nanoparticles decreased due to the presence of proteins in the environment, while its size increased. After a while, when the zeta potential was fixed, the nanoparticle re-generated and remained at a constant particle size as specified in the stability study. As a result of this study, it was observed that the particle size and polydispersity indices of the formulations increased as they approached 24 hours.

Figure 4 shows examples of polyacrylamide gels. Polyacrylamide gel electrophoresis studies were also conducted in polyacrylamide gel, as it is a more sensitive system to small particles of siRNA.



C: Control

Figure 4. Electrophoretic action of siRNA loaded with ionic interaction to Chi-GA-DAPC-MPEG-NMDA in 5% FBS in polyacrylamide gel

Malcolm et al.'s study found an increase in particle size and polydispersity index of nanoparticle-siRNA complexes in serum and nanoparticle-siRNA aggregation. The study found similar results in environments with 0.5% and 1% FBS. The zeta potential of the nanoparticles also changed, but it was not of high value that affected stability⁴⁸. However, in the medium containing 5% FBS, the nanoparticles showed relatively different properties due to increased protein concentration. The study found that formulations with larger particle sizes and polydispersity indices increased over 24 hours. Polyacrylamide gel electrophoresis studies showed that all formulations maintained siRNA integrity for 24 hours. Katas et al. developed chitosan nanoparticle formulations with smaller sizes to eliminate siRNA properties, which are rapidly metabolized and taken into cells. These formulations were completely broken down after 72 hours of application in serum²¹. In our studies with Chi-GA-DAPC-MPEG-NMDA nanoparticle formulation, we found that siRNA integrity was maintained for 24 hours.

As a result, nanoparticle formulations prepared from modified chitosan polymers were successfully developed in this study, in which nanoparticle systems containing siRNA were prepared and evaluated. As a result of the characterization studies, it has been determined that the ideal formulations obtained can be used in the treatment of HD intranasal route and as gene therapy due to its gene silencing effect. It has been determined that the obtained formulations have the desired particle size, zeta potential and particle size distribution and maintain their stability for a long time. The formulation showed a high rate of siRNA loading capacity. At the same time, it maintained siRNA integrity for 24 hours. The developed formulation is promising in the treatment of HD.

STATEMENT OF ETHICS

Ethics approval is not required in this study, as no human and experimental animal samples are involved.

CONFLICT OF INTEREST STATEMENT

The authors declare no conflict of interest.

AUTHOR CONTRIBUTIONS

Emre Şefik ÇAĞLAR, Emine Büşra EKER FİDAN, Mehmet Koray GÖK collected data, analyzed and interpreted results, and prepared the initial manuscript. Emre Şefik ÇAĞLAR, Mehmet Koray GÖK, Neslihan ÜSTÜNDAĞ OKUR, Saadet Kevser PABUCCUOĞLU, and Erdal CEVHER participated in the final version of the text. Erdal CEVHER supervised the project.

FUNDING SOURCES

This project was supported by TUBITAK Project No: 218S628.

ACKNOWLEDGMENTS

This study was generated from the PhD thesis of Emre Şefik Çağlar.

REFERENCES

1. Ross CA, Poirier MA. Protein aggregation and neurodegenerative disease. *Nat Med*, 2004;10(7):10-17. Doi: 10.1038/nm1066
2. Richards RI. Dynamic mutations: a decade of unstable expanded repeats in human genetic disease. *Hum Mo Genet*, 2001;10(20):2187-2194. Doi: 10.1093/hmg/10.20.2187
3. Ross CA, Tabrizi SJ. Huntington's disease: from molecular pathogenesis to clinical treatment. *Lancet Neuro*, 2011;10(1):83-98. Doi: 10.1016/S1474-4422(10)70245-3
4. Godinho BMDC, Ogier JR, Darcy R, O'Driscoll CM, Cryan FJ. Self-assembling modified β - cyclodextrin nanoparticles as neuronal siRNA delivery vectors: focus on Huntington's disease. *Mol Pharm*, 2013;10(2):640-649. Doi: 10.1021/mp3003946
5. Roos RAC. Huntington's disease: a clinical review. *Orphanet J Dis*, 2010;20(5):40. Doi: 10.1186/1750-1172-5-40
6. Videnovic A. Treatment of Huntington disease. *Curr Treat Options Neurol*, 2013;15(4):424-438. Doi: 10.1007/s11940-013-0219-8
7. Stefani G, Slack FJ. Small non-coding RNAs in animal development. *Nat Rev Mol Cell Biol*, 2008;9:219-230. Doi: <https://doi.org/10.1038/nrm2347>
8. He L, Hannon GJ. MicroRNAs: small RNAs with a big role in gene regulation. *Nat Rev Genet*, 2004;5:522-531. Doi: 10.1038/nrg1379
9. Zamore PD, Tuschl T, Sharp PA, Bartel DP. RNAi: double-stranded RNA directs the ATP-dependent cleavage of mRNA at 21 to 23 nucleotide intervals. *Cell*, 2000;101(1):25-33. Doi: 10.1016/S0092-8674(00)80620-0
10. Martinez J, Patkaniowska A, Urlaub H, Lührmann R, Tuschl T. Single-stranded antisense siRNAs guide target RNA cleavage in RNAi. *Cell*, 2002;110(5):563-574. Doi: 10.1016/S0092-8674(02)00908-X
11. Bernkop-Schnürch A, Dünnhaupt S. Chitosan-based drug delivery systems. *Eur J Pharm Biopharm*, 2012;81(3):463-469. Doi: 10.1016/j.ejpb.2012.04.007
12. Ezhilarasan D, Shree Harini K. Nanodrug delivery: strategies to circumvent nanoparticle trafficking by Kupffer cells in the liver. *J Drug Deliv Sci Technol*, 2023;86:104731. Doi: 10.1016/j.jddst.2023.104731
13. Fan MMY, Raymond LA. N-methyl-D-aspartate (NMDA) receptor function and excitotoxicity in Huntington's disease. *Prog Neurobiol*, 2007;81(5-6):272-293. Doi: 10.1016/j.pneurobio.2006.11.003
14. Sava V, Fihurka O, Khvorova A, Sanchez-Ramos J. Enriched chitosan nanoparticles loaded with siRNA are effective in lowering Huntington's disease gene expression following intranasal administration. *Nanomed*, 2020;24102119. Doi: 10.1016/j.nano.2019.102119
15. Eker Fidan EB, Bal K, Şentürk S, Kaplan Ö, Demir K, Gök MK. Enhancing gene delivery efficiency with amphiphilic chitosan modified by myristic acid and tertiary amino groups. *Int J Biol Macromol*, 2024;282(1):136775. Doi: 10.1016/j.ijbiomac.2024.136775
16. Gök MK, Demir K, Cevher E, Özgümiş S, Pabuccuoğlu S. Effect of the linear aliphatic amine functionalization on *in vitro* transfection efficiency of chitosan nanoparticles. *Carbohydr Polym*, 2019;207:580-587. Doi: 10.1016/j.carbpol.2018.12.013
17. Ahmed T, Aljaeid B. Preparation, characterization, and potential application of chitosan, chitosan derivatives, and chitosan metal nanoparticles in pharmaceutical drug delivery. *Drug Des Devel Ther*, 2016;2016(10):483. Doi: 10.2147/DDDT.S99651

18. Üstündağ-Okur N, Gökçe EH, Bozbiyık Dİ, Eğrilmez S, Özer Ö, Ertan G. Preparation and *in vitro-in vivo* evaluation of ofloxacin loaded ophthalmic nano structured lipid carriers modified with chitosan oligosaccharide lactate for the treatment of bacterial keratitis. *Eur J Pharm Sci*, 2014;63:204-215. Doi: 10.1016/j.ejps.2014.07.013
19. Hazzah HA, Farid RM, Nasra MMA, EL-Massik MA, Abdallah OY. Lyophilized sponges loaded with curcumin solid lipid nanoparticles for buccal delivery: development and characterization. *Int J Pharm*, 2015;492(1-2):248-257. Doi: 10.1016/j.ijpharm.2015.06.022
20. Abdul M, Raja G, Katas H. Stability, intracellular delivery, and release of siRNA from chitosan nanoparticles using different cross-linkers. *Plos One*, 2015;10(6):1-19. Doi: 10.1371/journal.pone.0128963
21. Katas H, Alpar HO. Development and characterisation of chitosan nanoparticles for siRNA delivery. *J Control Release*, 2006;115(2):216-225. Doi: 10.1016/j.jconrel.2006.07.021
22. Muthu MS, Feng S-S. Pharmaceutical stability aspects of nanomedicines. *Nanomed*, 2009;4(8):857-860. Doi: 10.2217/nnm.09.75
23. Gedde UW. Thermal analysis of polymers. In: *Polymer physics*. Springer, Dordrecht: Netherlands. 1999. pp. 217-237. Doi: 10.1007/3-540-06552-0_2
24. Gao K, Jiang X. Influence of particle size on transport of methotrexate across blood brain barrier by polysorbate 80-coated polybutylcyanoacrylate nanoparticles. *Int J Pharm*, 2006;310(1-2):213-219. Doi: 10.1016/j.ijpharm.2005.11.040
25. Olivier JC. Drug transport to brain with targeted nanoparticles. *NeuroRx*, 2005;2:108-119. Doi: 10.1602/neurorx.2.1.108
26. Patel S, Chavhan S, Soni H, Babbar AK, Mathur R, Mishra AK, et al. Brain targeting of risperidone-loaded solid lipid nanoparticles by intranasal route. *J Drug Target*, 2011;19(6):468-474. Doi: 10.3109/1061186X.2010.523787
27. Gratton SEA, Ropp PA, Pohlhaus PD, Luft JC, Madden VJ, Napier ME, DeSimone JM. The effect of particle design on cellular internalization pathways. *Proc Natl Acad Sci USA*, 2008;105(33):11613-11618. Doi: 10.1073/pnas.0801763105
28. Hillaireau H, Couvreur P. Nanocarriers' entry into the cell: relevance to drug delivery. *Cell Mol Life Sci*, 2009;66:2873-2896. Doi: 10.1007/s00018-009-0053-z
29. Muntimadugu E, Dhommati R, Jain A, Challa VGS, Shaheen M, Khan W. Intranasal delivery of nanoparticle encapsulated tarenflurbil: a potential brain targeting strategy for Alzheimer's disease. *Eur J Pharm Sci*, 2016;92:224-234. Doi: 10.1016/j.ejps.2016.05.012
30. Etame AB, Smith CA, Chan WCW, Rutka MD JT. Design and potential application of PEGylated gold nanoparticles with size-dependent permeation through brain microvasculature. *Nanomed*, 2011;7(6):992-1000. Doi: 10.1016/j.nano.2011.04.004
31. Hanada S, Fujioka K, Inoue Y, Kanaya F, Manome Y, Yamamoto K. Cell-based *in vitro* blood-brain barrier model can rapidly evaluate nanoparticles' brain permeability in association with particle size and surface modification. *Int J Mol Sci*, 2014;15(2):1812-1825. Doi: 10.3390/ijms15021812
32. Godinho BMDC, Ogier JR, Darcy R, O'Driscoll CM, Cryan JF. Self-assembling modified β -cyclodextrin nanoparticles as neuronal siRNA delivery vectors: focus on Huntington's disease. *Mol Pharm*, 2013;10(2):640-649. Doi: 10.1021/mp3003946
33. Van Woensel M, Wauthoz N, Rosière R, Mathieu V, Kiss R, Lefranc F, et al. Development of siRNA-loaded chitosan nanoparticles targeting Galectin-1 for the treatment of glioblastoma multiforme via intranasal administration. *J Control Release*, 2016;227:71-81. Doi: 10.1016/j.jconrel.2016.02.032

34. Jallouli Y, Paillard A, Chang J, Sevin E, Betbeder D. Influence of surface charge and inner composition of porous nanoparticles to cross blood-brain barrier *in vitro*. *Int J Pharm*, 2007;344(1-2):103-109. Doi: 10.1016/j.ijpharm.2007.06.023
35. Alihosseini F, Ghaffari S, Dabirsiaghi AR, Haghghat, S. Freeze-drying of ampicillin solid lipid nanoparticles using mannitol as cryoprotectant. *Braz J Pharm Sci*, 2015;51:797-802. Doi: 10.1590/S1984-82502015000400005
36. Abdelwahed W, Degobert G, Stainmesse S, Fessi, H. Freeze-drying of nanoparticles: formulation, process and storage considerations. *Adv Drug Deliv Rev*, 2006;58(15):1688-1713. Doi: 10.1016/j.addr.2006.09.017
37. Almalik A, Alradwan I, Kalam MA, Alshamsan A. Effect of cryoprotection on particle size stability and preservation of chitosan nanoparticles with and without hyaluronate or alginate coating. *Saudi Pharm J*, 2017;25(6):861-867. Doi: 10.1016/j.jpsps.2016.12.008
38. Gokce Y, Cengiz B, Yildiz N, Calimli A, Aktas Z. Ultrasonication of chitosan nanoparticle suspension: influence on particle size. *Colloids Surf A Physicochem Eng Asp*, 2014;462:75-81. Doi: 10.1016/j.colsurfa.2014.08.028
39. Fonte P, Soares S, Costa A, Andrade JC, Seabra V, Reis S, Sarmento B. Effect of cryoprotectants on the porosity and stability of insulin-loaded PLGA nanoparticles after freeze-drying. *Biomater*, 2012;2(4):329-339. Doi: 10.4161/biom.23246
40. Akbaba H, Demir Dora D, Kantarci AG. The effects of lyophilization and cryoprotectants on solid lipid nanoparticle-DNA systems. *Rom Biotechnol Lett*, 2017;22(6):13186-13195. Doi: 10.26327/RBL2017.05
41. Ball R, Bajaj P, Whitehead K. Achieving long-term stability of lipid nanoparticles: examining the effect of pH, temperature, and lyophilization. *Int J Nanomedicine*, 2016;2017(12):305-315. Doi: 10.2147/IJN.S123062
42. Zhang Y, Wang H, Stewart S, Jiang B, Ou W, Zhao G, He X. Cold-responsive nanoparticle enables intracellular delivery and rapid release of trehalose for organic-solvent-free cryopreservation. *Nano Lett*, 2019;19(12):9051-9061. Doi: 10.1021/acs.nanolett.9b04109
43. Almalik A, Alradwan I, Kalam MA, Alshamsan A. Effect of cryoprotection on particle size stability and preservation of chitosan nanoparticles with and without hyaluronate or alginate coating. *Saudi Pharm J*, 2017;25(6):861-867. Doi: 10.1016/j.jpsps.2016.12.008
44. Anchordoquy TJ, Jinxiang Y. Effects of moisture content on the storage stability of dried lipoplex formulations. *J Pharm Sci*, 2009;98(9):3278-3289. Doi: 10.1002/jps.21846
45. Üstündağ-Okur N, Yurdasiper A, Gündoğdu E, Gökçe Homan E. Modification of solid lipid nanoparticles loaded with nebigolol hydrochloride for improvement of oral bioavailability in treatment of hypertension: polyethylene glycol versus chitosan oligosaccharide lactate. *J Microencapsul*, 2016;33(1):30-42. Doi: 10.3109/02652048.2015.1094532
46. Carrillo C, Suñé JM, Pérez-Lozano P, García-Montoya E, Sarrate R, Fàbregas A, Ticó JR. Chitosan nanoparticles as non-viral gene delivery systems: determination of loading efficiency. *Biomed Pharmacother*, 2014;68(6):775-783. Doi: 10.1016/j.biopha.2014.07.009
47. Raval N, Jogi H, Gondaliya P, Kalia K, Tekade RK. Method and its composition for encapsulation, stabilization, and delivery of siRNA in Anionic polymeric nanoplex: an *in vitro- in vivo* assessment. *Sci Rep*, 2019;9:1-18. Doi: 10.1038/s41598-019-52390-4
48. Malcolm DW, Varghese JJ, Sorrells JE, Ovitt CE, Benoit DS. The effects of biological fluids on colloidal stability and siRNA delivery of a pH-responsive micellar nanoparticle delivery system. *ACS Nano*, 2018;12(1):187-197. Doi: 10.1021/acs.nano.7b05528